

# Electrostatic-assembly metallized nanoparticles network by DNA template

Aiguo Wu, Wenlong Cheng, Zhuang Li\*, Junguang Jiang, Erkang Wang\*

State Key Laboratory of Electroanalytical Chemistry, Chinese Academy of Sciences, Changchun Institute of Applied Chemistry, Changchun 130022, China

Received 8 June 2004; received in revised form 12 May 2005; accepted 12 May 2005

Available online 27 June 2005

## Abstract

Eighteen-nanometer gold and 3.5-nm silver colloidal particles closely packed by cetyltrimethylammonium bromide (CTAB) to form its positively charged shell. The DNA network was formed on a mica substrate firstly. Later, CTAB-capped gold or silver colloidal solutions were cast onto DNA network surface. It was found that the gold or silver nanoparticles metallized networks were formed owing to the electrostatic-driven template assembling of positive charge of CTAB-capped gold and silver particles on the negatively charged phosphate groups of DNA molecules by the characterizations of AFM, XPS and UV-vis. This method may provide a novel and simple way to studying nanoparticles assembly conjugating DNA molecules and offer some potential promising applications in nanocatalysis, nanoelectronics, and nanosensor on the basis of the fabricated metal nanoparticles network.

© 2005 Elsevier B.V. All rights reserved.

**Keywords:** DNA; Nanoparticle; Network; AFM; Self-assemble

## 1. Introduction

A key goal of nanosized science and technology is the innovation of protocols to the interactions, and the long-range order of various nanoparticles and clusters on different solid substrates. It can offer some novel properties of materials and devices based on the mesoscopic physics, chemistry and catalysis. Biometric “bottom-up” approaches are popularly being explored for the self-assembly of functional devices by molecular and nanoparticulate construct units [1–3]. Among the biological templates that can be used as candidates in nanostructure systems [4–6], DNA molecules, in particular, are promising templates for assemblies from several nanometers up to several tens of micrometers. In addition, the columnar double-helix structure of DNA molecules together with the ability to the negative charge in phosphate backbone of DNA molecules to fastening metal nanoparticles makes them become ideal templates for growing nanowires or

other intricate nanostructures by binding together metal or semiconductor nanoparticles [4–6].

To date, both covalent and non-covalent self-assembly strategies have been widely used to assemble nanoscale inorganic particles into two- and three-dimensional mesoscopic and macroscopic structures using DNA since Coffey et al. took advantage of DNA as a building block for various nanostructures [6–15]. Braun et al. have reported an example that a silver nanowire which is formed using the DNA as a skeleton [6]. Current-voltage measurement showed the potential use of these nanowires. Subsequently, some groups have also described some methods of DNA-based template Pd nanoclusters, Au nanoclusters, Pt nanoclusters and CdS nanometer network, etc. [7–10]. Mirkin et al. and Alivisatos et al. have done pioneering studies on gold and CdS nanoparticles using DNA base-pairing principle [11,12]. Sastry et al. have reported the electrostatic assembly of lysine-packed gold DNA-inspired linear or cluster superstructures and Torimoto group described the electrostatic assembly of CdS nanocrystal chains along with DNA strand templates [13–15]. These strategies have advantages and disadvantages relying on the targeted nanoparticle-based components. A

\* Corresponding authors. Tel.: +86 431 5262057; fax: +86 431 5689711.

E-mail addresses: [zli@ns.ciac.jl.cn](mailto:zli@ns.ciac.jl.cn) (Z. Li), [ekwang@ns.ciac.jl.cn](mailto:ekwang@ns.ciac.jl.cn) (E. Wang).

method of the nanoparticles network constructed which includes the good stability and narrow size distribution of the nanoparticle building blocks and large scale of the extended structure would be greatly advantageous [16].

Herein, we report a DNA-mediated electrostatic assembly of CTAB-encapsulated gold and silver colloidal nanoparticles into two-dimensional mesoscopic network on mica substrates. Comparing with other methods, this approach has some advantages: First, the building block, CTAB-encapsulated noble metal (gold and silver) nanoparticles have good stability and are well dispersed owing to CTAB decreasing the activity of the surface atoms of the colloidal particles avoiding their aggregation. Second, this metallized network has large scale (principally, it can reach the whole area of the mica substrate). Third, this metallized network owns some controllable parameters since the diameter of noble metal nanoparticles is selectable and the frames of DNA network are tailorable by choosing conditions [17–19]. Fourth, the building blocks of this strategy are various. Although here we select Au and Ag, we can choose other nanoparticles act as the constructed units, such as metal nanoparticles, Pt, Pd and other suitable semiconductor quantum dots. Thus, it may pave a simple approach to nanoparticles assembly on the basis of the DNA template. Furthermore, we discuss in detail the possible applications in sensing and surface enhanced Raman spectroscopy (SERS) fields according to some novel progress on the assembled nanoparticles array.

## 2. Experimental

### 2.1. Preparing metal nanoparticles and metallized networks

Cetyltrimethylammonium bromide (CTAB,  $(\text{CH}_3(\text{CH}_2)_{15}\text{N}(\text{CH}_3)_3)\text{Br}$ , Beijing Chemicals), citrate trisodium (Beijing Chemicals),  $\text{NaBH}_4$  (Acros),  $\text{AgNO}_3$  (Beijing Chemicals) and  $\text{HAuCl}_4$  (Beijing Chemicals) were used as received. Double strands DNA pBR322/pstI (4361 bp) solution was purchased from Beijing Branch of Sino-American Biotechnology Co. (Beijing, China). All other chemicals were of reagent grade and used as received. Solutions were prepared using Millipore Milli-Q purified water. Eighteen-nanometers of gold and 3.5-nm of silver nanoparticles colloidal solutions were synthesized and encapsulated with CTAB as described below. The gold colloidal nanoparticles solution were prepared by citrate trisodium (3%, 1 mL) reduction of  $\text{HAuCl}_4$  (0.1%, 10 mL) in 50 mL aqueous solution as reported elsewhere [20a]. After the solution was cooled, the gold particles was encapsulated with CTAB solution to yield an overall CTAB concentration in the colloidal solution of  $2.5 \times 10^{-5}$  mol/L and form positively charged shell. The reduction of  $\text{AgNO}_3$  (5.0 mM, 60 mL) by sodium borohydride (0.4 M, 10 mL) in the presence of  $2.3 \times 10^{-5}$  mol/L CTAB gave a stable aqueous dispersion of

3.5 nm of silver nanoparticles with positively charged shell [21b]. The hydrophilic tails are exposed towards outside because CTAB is an oily molecules, between of them exist in the hydrophobic interactions, which occur when oily molecules pack together to limit their exposure to water [16]. Hence, these CTAB molecules adsorbed on gold and silver cores formed interdigitated bilayer structure [21]. There are two steps to get the metallized network. First, a 3–15  $\mu\text{L}$  of diluted 60–320 ng/ $\mu\text{L}$  DNA pBR322/pstI sample solution was dropped on freshly cleaved mica with pipette tips and spread over the surface about 10 mm of the diameter. After standing on the substrates for 3–5 min, the sample was dried 2 h in the desiccator and DNA network was formed on the mica surface [17–19]. Second, CTAB-capped colloidal gold or silver particles solutions were cast onto DNA network surfaces. After standing on the surfaces for about 30 min, the sample was blown off in air and stored in the desiccator until use. The electrostatic self-assembling of positively charged colloidal gold and silver nanoparticles along the negatively charged fringes of DNA network was formed.

### 2.2. AFM imaging

Tapping-mode AFM was operated in air using a Multi-mode scanning probe microscope (SPM) with a Nanoscope IIIa Controller and Nanoscope Extender (Digital Instruments, Santa Barbara, CA, USA). The J-Scanner and silicon micro-cantilevers (Digital Instruments, resonance frequency 150–350 kHz) were employed for all measurements. The  $512 \times 512$  pixel images were obtained with a scan rate range of 1–2.5 Hz. Images were only processed by flattening using nanoscope software to remove background slope. Heights relative to the substrate were acquired from topographic profiles. The mean roughness ( $R_a$ ) of the mica substrates was typically no greater than 0.06 nm.

### 2.3. UV-vis spectra

The optical properties of the DNA solution, the CTAB-encapsulated gold, CTAB-coated silver nanoparticle colloidal solution, CTAB-encapsulated gold–DNA and CTAB-capped silver–DNA complex solutions were monitored on a CARY 500 (USA) spectrophotometer.

### 2.4. XPS

X-ray photoelectron spectroscopy (XPS) measurements were made in a Vacuum Generators ESCALab MK II instrument (VG Co., UK). 300 W Mg X-rays ( $h\nu = 1253.6$  eV) were used to excite photoelectrons from Au 4f, Ag 3d and C 1s core level.

## 3. Results and discussion

UV-vis spectra of the CTAB-encapsulated gold–DNA and silver–DNA solutions were shown in Figs. 1 and 2,

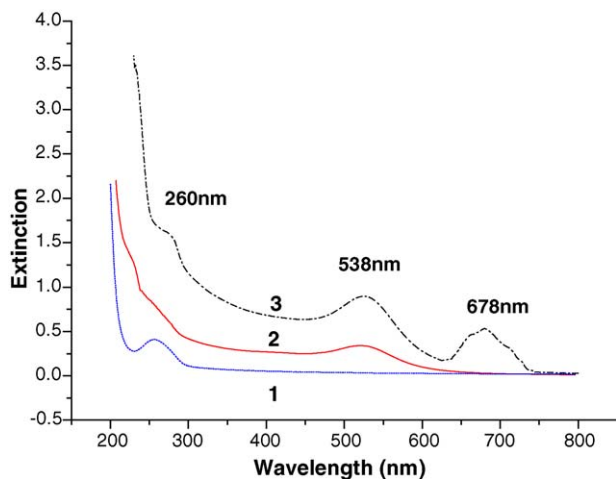


Fig. 1. UV-vis spectra of DNA solution (curve 1), CTAB-encapsulated gold nanoparticle solution (curve 2) and DNA-CTAB-encapsulated gold nanoparticle mixed solution (curve 3).

respectively. In Fig. 1, curves 1–3 in the main part of this figure correspond to spectra recorded from DNA solution, the CTAB-encapsulated gold colloidal solution and the CTAB-encapsulated gold–DNA solution, respectively. It is found that there is a widening of the surface plasmon resonance on coordination of the CTAB-encapsulated gold nanoparticles with the DNA molecules (compare curves 1 and 2 with 3) and the degree of widening is considerably higher. Some interesting features are found which may be explained as follows. A strong resonance is seen at 538 nm in both the CTAB-encapsulated gold nanoparticles and the DNA molecules conjugated CTAB-encapsulated gold nanoparticles. This resonance peak is due to the excitation of surface plasmon vibrations in the gold nanoparticles and is responsible for the wine-red color of the nanoparticle solutions [22]. This resonance peak is clearly absent in the DNA solution

(in curve 1) except the peak of 260 nm, which is the characteristic peak of DNA. Additionally to the resonance peak at 538 nm, the DNA sample conjugated CTAB-capped gold nanoparticles shows another resonance peak at 678 nm. It is well known that aggregation of noble metal nanoparticles such as gold and silver into quasi-two-dimensional superstructures causes the appearance of a longitudinal surface plasmon resonance red shifted with respect to the transverse component (in this case, the 538 nm resonance peak) [13,14,22]. (It should be noted that in some cases, the peak at 678 nm can not find and only have a wide peak which is a convolution peak of the red-shift peak for the plasmon resonance peak and its original resonance peak of the gold nanoparticles if the assembled structures are not close-packed style [1d].) The appearance of the longitudinal plasmon resonance peak at 678 nm in the DNA-gold nanoparticle conjugation is thus strongly indicative of assembly of the CTAB-coated gold nanoparticles in extended structures driven by the underlying DNA template. Because the optical properties of colloidal gold solutions change when the nanoparticles aggregate, the main feature being the growth of a long wavelength resonance owing to overlapping of the surface plasmon modes from neighboring nanoparticles [13,14,22]. Attractively electrostatic interaction between the positive charges in the CTAB-encapsulated gold nanoparticles and the negative charges on the phosphate groups of the DNA template molecules stimulates the assembly of the gold nanoparticles into close-packed, network structures inferred from the UV-vis measurements. The DNA molecules thus act as a bridge interaction and drive the CTAB-encapsulated gold nanoparticles with positive charge assembling into metallized network superstructures on mica substrates.

Similarly, the UV-vis spectra obtained are shown in Fig. 2 of curves 1–3 in the main part of the figure corresponding to spectra recorded from the DNA solution, CTAB-capped silver nanoparticles solution and the DNA-Ag capped by CTAB complexes solution orderly. In curve 1, a strong absorption peak at ca. 260 nm is observed that corresponds to the characteristic peak of DNA solutions. In the spectra of curve 2, a strong absorption at ca. 410 nm is observed that corresponds to the excitation of surface plasmon vibrations in the silver particles [23–25]. The peak at 510 nm in curve 3 is due to the appearance of a longitudinal plasma resonance peak and is a consequence of the overlap of the dipole resonance between neighboring silver particles except the peaks of both 260 nm and 410 nm. The appearance of the longitudinal plasmon resonance peak at 510 nm in the DNA-Ag nanoparticle complexes is thus strongly indicative of assembly of the CTAB-capped silver nanoparticle in extended structures driven by the DNA template [23–25]. Because the optical properties of colloidal silver solutions change when the nanoparticles aggregate, the main feature being the growth of a long wavelength resonance owing to the overlap of the surface plasmon modes from neighboring nanoparticles (it is similar to the gold nanoparticles case).

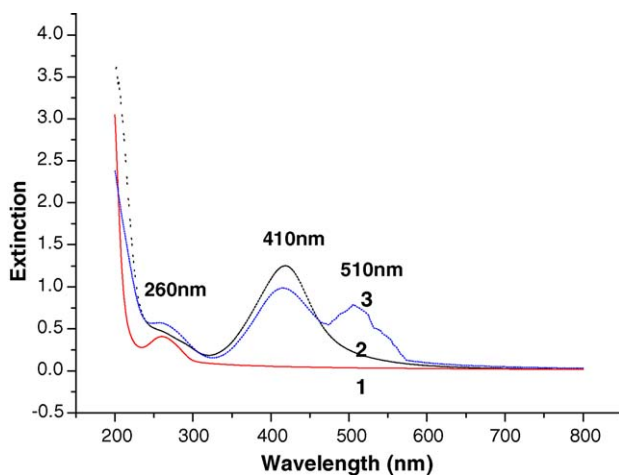


Fig. 2. UV-vis spectra of DNA solution (curve 1), CTAB-capped silver nanoparticle solution (curve 2) and DNA-CTAB-capped silver nanoparticle mixed solution (curve 3).

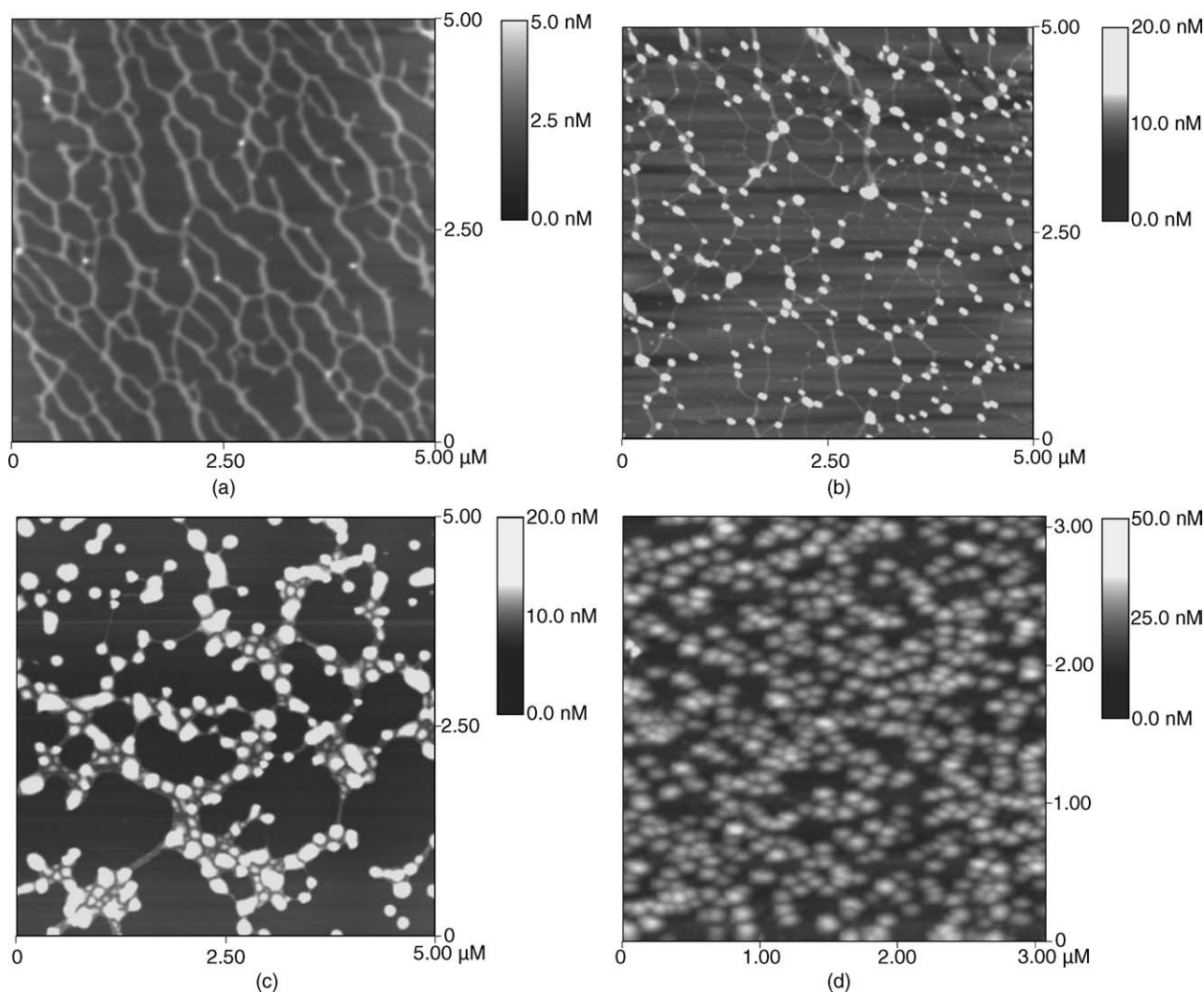


Fig. 3. (a) AFM images of DNA network, DNA: 200 ng/ $\mu$ L, 6  $\mu$ L. (b)–(d) AFM images of the interaction between different CTAB-encapsulated gold nanoparticle solutions and DNA. (b) DNA concentration: 130 ng/ $\mu$ L, 3  $\mu$ L, CTAB-encapsulated gold nanoparticle solution 5  $\mu$ L. (c) DNA concentration: 80 ng/ $\mu$ L, 3  $\mu$ L, CTAB-encapsulated gold nanoparticle solution 12  $\mu$ L. (d) DNA concentration: 300 ng/ $\mu$ L, 3  $\mu$ L, CTAB-encapsulated gold nanoparticle solution 17  $\mu$ L.

Direct evidence of the formation of network assemblies of CTAB-coated gold and silver nanoparticles driven by the DNA template and indirectly inferred from UV-vis results was acquired from the atomic force microscopy (AFM) measurements. The AFM image obtained from the as-prepared DNA network is shown in Fig. 3a. It is shown that the DNA networks have formed orderly. The DNA networks are extremely stable and do not cause the movement of the DNA strands on the substrates, even if they are repeatedly scanned many times. Fig. 3b–d show the AFM images of the interactions both the different concentrations of the DNA solutions and the distinct quantitative of 18 nm CTAB-encapsulated gold nanoparticles.

These images clearly confirm that CTAB-encapsulated gold nanoparticles are highly specific assembled by DNA network template. It is found that the nanoparticles, which are assembled on the DNA network, become more and more

dense along the fringe of DNA network on mica substrates with the increasing of the quantitative of gold nanoparticles. It proves that the CATB-encapsulated gold nanoparticles are assembled by the DNA network template due to electrostatic attractive interaction. Fig. 4 shows the image of the interaction between DNA and silver nanoparticles, which further validates nanoparticles to be specially assembled by DNA template. In Fig. 4, the measured sizes of silver nanoparticles and DNA strands are larger than their contour sizes due to the convoluted interaction of AFM tip and the samples. We think it is the widened effect of AFM tips. The matter of fact, the measured total height of the silver and DNA strands is 3.9–5.3 nm, which is consistent with their contour total height 5.5 nm. There are similar results in CTAB-capped gold nanoparticles conjugating DNA system, which the CTAB-capped gold nanoparticles are also widened by AFM tips.

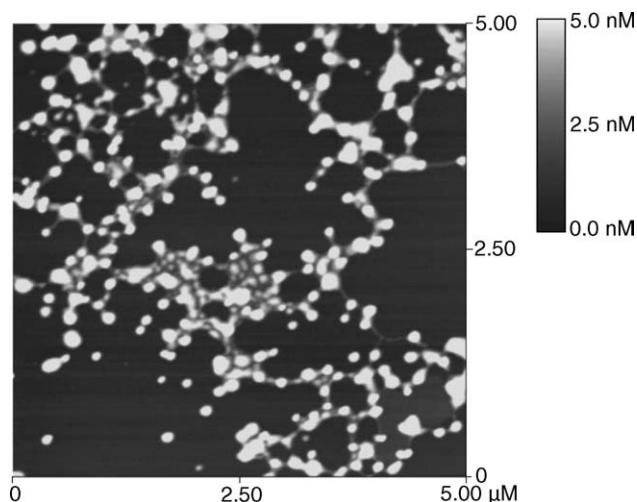


Fig. 4. AFM images of the interaction between DNA solution and CTAB-capped silver nanoparticle solution: DNA concentration, 90 ng/ $\mu$ L, 5  $\mu$ L; CTAB-capped silver nanoparticle solution, 8  $\mu$ L.

A chemical analysis of these metallized DNA networks were done using XPS and the Au 4f, Ag 3d and C 1s core level spectra were recorded (shown in Fig. 5a–c). Fig. 5a showed the Au 4f core level spectrum, which could be satisfactorily fit to a single spin-orbit pair. The binding energy (BE) of the 4f component is recorded to be 83.8 eV and is characteristic of metallic Au [26]. Fig. 5b shows the Ag<sub>3d</sub> core level spectrum, which can be satisfied, fit to a single spin-orbit pair. The binding energy (BE) of the Ag 3d component is recorded to be 368.2 and 371.2 eV is characteristic of metallic Ag [24]. The C 1s spectrum can be resolved into two chemically different components at 285.2 and 288.3 eV (shown in Fig. 5c). The lower BE component in the C 1s spectrum is assigned to carbons in the DNA sugars and bases while the higher BE component arises owing to electron emission from carbons coordinated to the functional groups in the gold or silver surface adsorbed CTAB molecules [14].

These results indicate that this approach is suitable to controlling the two-dimensional arrangement of metal nanoparticles on a large scale on solid substrates. It is noted that this

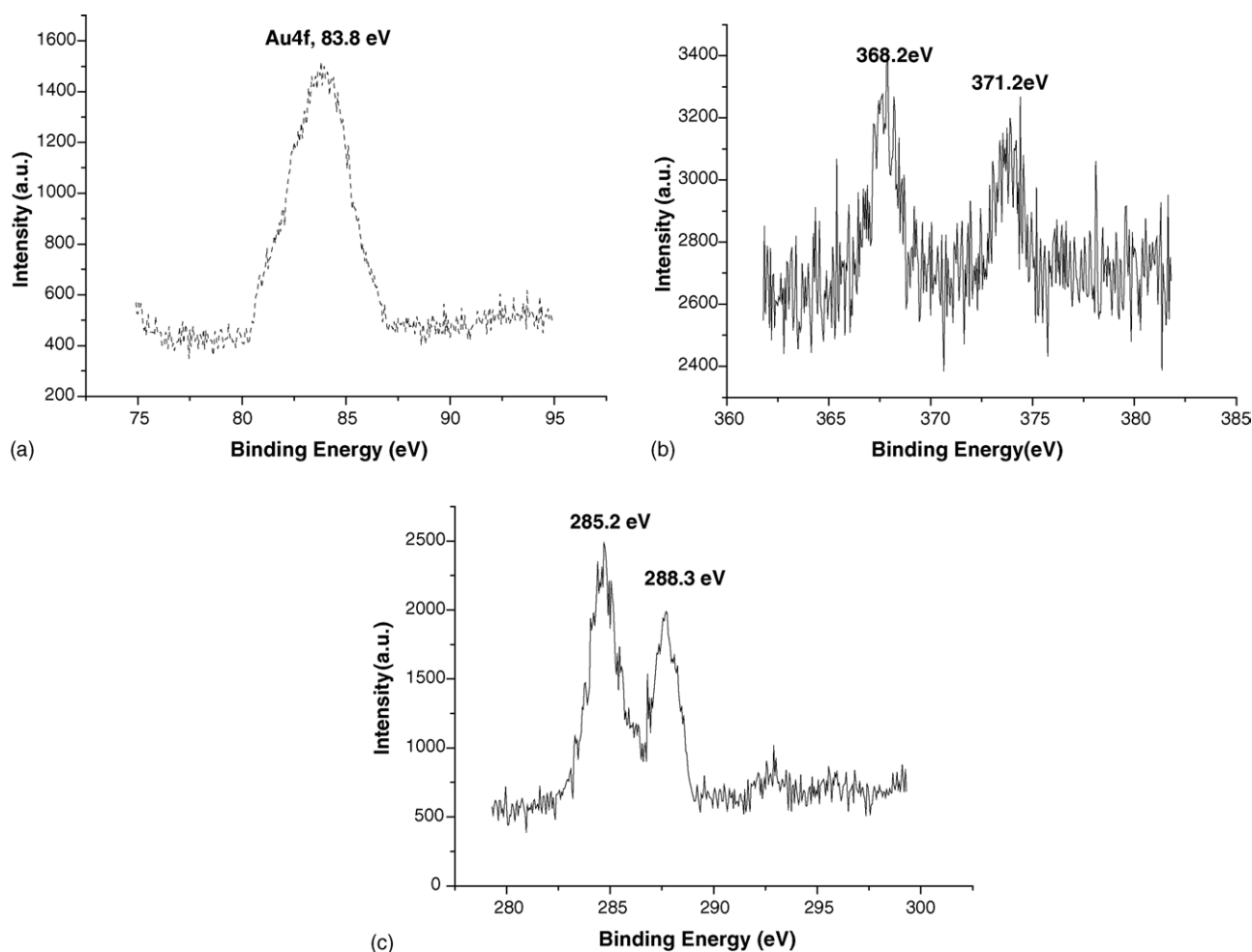


Fig. 5. XPS spectra of the Au 4f, Ag 3d and C 1s core level recorded from the DNA and CTAB-encapsulated gold nanoparticle mixed solutions and CTAB-capped silver-DNA solutions: (a) Au 4f; (b) Ag 3d; (c) C 1s.

fabricated approach to the nanoparticle network can be extended to other systems for example Pt, Pd, Cu, CdS, CdSe, ZnO, ZnS, ZnSe and CdTe so on [27]. The nanoparticles network can be adjusted by controlling the DNA network template because the DNA network can be covered over the whole solid supports and formed on various solid substrates such as mica, glass, sapphire, HOPG and SiO<sub>2</sub>/Si [17–19]. Moreover, some improvements in the methodology, in particular, the binding strength of DNA and the CTAB modified nanoparticles and the mesh diameter of the DNA network template, are necessary for this method to be used in widely applicable fields. If the condition is controlled, the positively modified nanoparticles in conjugation with DNA network templates will allow us to assemble them into large-scale integration and different types of circuits with a defined suprastructure [17–19].

The nanoparticle networks or superstructures assembled on various solid substrates are expected to produce systems of electronically and optical properties. Nanoparticulate gold or silver monolayer network/superstructures assembled on all kinds of solid supports have been widely used for a photoelectrochemical sensor, for the electrochemical sensing of hydroquinones by their preconcentration in some receptor binding sites, for a sensory application in the ion-sensitive field-effect transistors (ISFET) to provide interesting transducers and for an optical application as a SERS substrate [27,28]. For example, Willner group elaborated the gold nanoparticles monolayer array for the electrochemical sensing of various neurotransmitters, dopamine, dihydroxyphenylacetic acid, and adrenaline [27a]. A more recent study coming from one of our groups, found that silver nanoparticles assembled on the DNA network template on a modified mica surface could be used for a SERS substrate. In that case, nanoparticles silver labeled with dyes-R6G of  $1 \times 10^{-8}$  M produced a clear enhanced effect at  $1650 \text{ cm}^{-1}$  [28]. Such great Raman enhancement was obtained on the nanoparticulate silver self-assembled network, which is used for optical sensing besides its electronically sensing applications. That nano-Ag particles network is so similar to our present work, thus it provides a direct evidence for our Au or Ag nanoparticle networks in the application of optical sensing.

In summary, we fabricate a two-dimensional metal nanoparticles network using DNA network as a template via electrostatic attraction interaction. We believe that this simple method not only has great potential applications in nanoscale assembly using DNA template, but also has potential promising applications in nanocatalysis, nanooptoelectronics, and nanosensor for the fabricated metal nanoparticles network.

## Acknowledgements

This work was supported by the National Natural Science Foundation of China (Nos. 30070417 and 20275037).

## References

- [1] (a) C.M. Niemeyer, *Curr. Opin. Chem. Biol.* 4 (2000) 609; (b) C.M. Niemeyer, *Angew. Chem. Int. Ed* 40 (2001) 4128; (c) E. Dunjardin, S. Mann, *Adv. Mater.* 14 (2002) 775; (d) G. Wang, R. Murray, *NanoLett.* 4 (2004) 95.
- [2] M. Sastry, *Curr. Sci.* 78 (2000) 1089.
- [3] S. Henrichs, C.P. Collier, R.J. Saykally, J.R. Heath, *J. Am. Chem. Soc.* 122 (2000) 4077.
- [4] (a) W. Shenton, T. Douglas, M. Young, G. Stubbs, S.T. Mann, *Adv. Mater.* 11 (1999) 253; (b) J.L. Coffey, S.R. Bigham, X. Li, R.F. Pinizzotto, Y.G. Rho, R.M. Pirtle, I.L. Pirtle, *Appl. Phys. Lett.* 69 (25) (1996) 3851; (c) A. Wu, Z. Li, H. Zhou, E. Wang, *Superlatt. Microstruct.* 37 (2005) 151.
- [5] W. Shenton, D. Pum, U.B. Sleytr, S. Mann, *Nature* 389 (1997) 585.
- [6] E. Braun, Y. Eichen, U. Sivan, G. Ben-Yoseph, *Nature* 391 (1998) 775.
- [7] W.E. Ford, O. Harnack, A. Yasuda, J.M. Wessels, *Adv. Mater.* 13 (2001) 1793.
- [8] C.A. Berven, L. Clarke, J.L. Mooster, M.W. Wybourne, J.E. Hutchison, *Adv. Mater.* 13 (2000) 109.
- [9] J. Richter, R. Seidel, R. Kirsch, M. Mertig, W. Pompe, J. Plaschke, H.K. Schackert, *Adv. Mater.* 12 (2000) 507.
- [10] I. Willner, F. Patolsky, J. Wasserman, *Angew. Chem. Int. Ed* 40 (2001) 1861.
- [11] (a) C.A. Mirkin, R.L. Letsinger, R.C. Mucic, J.J. Storhoff, *Nature* 382 (1996) 607; (b) Y. Weizmann, F. Patolsky, I. Popov, I. Willner, *NanoLett.* 4 (2004) 787.
- [12] A.P. Alivisatos, K.P. Johnsson, X. Peng, T.E. Wilson, C.J. Loweth, M.P. Bruchez Jr., P.G. Schultz, *Nature* 382 (1996) 609.
- [13] M. Sastry, A. Kumar, S. Datar, C.V. Dharmadhikari, K.N. Ganesh, *Appl. Phys. Lett.* 78 (2001) 2943.
- [14] A. Kumar, M. Pattarkine, M. Bhadbhade, A.B. Mandale, K.N. Ganesh, S.S. Datar, C.V. Dharmadhikari, M. Sastry, *Adv. Mater.* 13 (2001) 341.
- [15] (a) T. Torimoto, M. Yanashita, S. Kuwabata, T. Sakata, H. Meri, H. Yoneyama, *J. Phys. Chem. B* 103 (1999) 8799; (b) C.M. Niemeyer, *Science* 297 (2002) 62.
- [16] J. Alper, *Science* 295 (2002) 2396.
- [17] T. Kanno, T. Tanaka, N. Miyoshi, T. Kawai, *Jpn. J. Appl. Phys.* 39 (2000) 269.
- [18] (a) A. Wu, Z. Li, L. Yu, H. Wang, E. Wang, *Anal. Sci.* 17 (2001) 583; (b) A. Wu, Z. Li, H. Zhou, J. Zheng, E. Wang, *Analyst* 127 (2002) 585; (c) A. Wu, Z. Li, L. Yu, H. Wang, E. Wang, *Ultramicroscopy* 92 (3–4) (2002) 201; (d) A. Wu, Z. Li, E. Wang, *Anal. Sci.* 20 (2004) 1083.
- [19] J. Ye, K. Umemura, M. Ishikawa, R. Kuroda, *Anal. Biochem.* 281 (2000) 21.
- [20] (a) G. Frens, *Nature* 241 (1973) 20; (b) T. Yonezawa, S. Onoue, N. Kimizuka, *Langmuir* 16 (2000) 5218.
- [21] (a) C. Patil, K.S. Mayya, S.D. Pradhan, M. Sastry, *J. Am. Chem. Soc.* 119 (1997) 9281; (b) W. Cheng, S. Dong, E. Wang, *Electrochem. Commun.* 4 (2002) 412.
- [22] V. Patil, R.B. Malvankar, M. Sastry, *Langmuir* 15 (1999) 8197.
- [23] P. Mulvaney, *Langmuir* 12 (1996) 788.
- [24] A. Gole, S.R. Sainkar, M. Sastry, *Chem. Mater.* 12 (2000) 1234.
- [25] M.D. Malinsky, K.L. Kelly, G.C. Schatz, R.P.V. Dwyne, *J. Am. Chem. Soc.* 123 (2001) 1471.
- [26] S.R. Johnson, S.D. Evans, S.W. Mahon, A. Ulman, *Langmuir* 13 (1997) 51.

- [27] (a) M. Lahav, A.N. Shipway, I. Willner, *J. Chem. Soc., Perkin Trans.* 2 (1999);  
(b) M. Lahav, T. Gabriel, A.N. Shipway, I. Willner, *J. Am. Chem. Soc.* 121 (1999) 258;  
(c) A.N. Shipway, M. Lahav, R. Blonder, I. Willner, *Chem. Mater.* 11 (1999) 13;  
(d) A.B. Kharitonov, A.N. Shipway, I. Willner, *Anal. Chem.* 71 (1999) 5441;  
(e) E. Katz, I. Willner, *Angew. Chem. Int. Ed* 43 (2004) 6042, and references therein.
- [28] G. Wei, H. Zhou, Z. Liu, Y. Song, L. Wang, L. Sun, Z. Li, *J. Phys. Chem. B.* 109 (2005) 8738.